Direct observation of structural and defect evolution in C-rich SiC using in situ helium ion microscopy

Wen Liu, Laifei Cheng, Xiaoqiang Li and Yiguang Wang*

* *Science and Technology on Thermostructural Composite Materials Laboratory, Northwestern Polytechnical University, Xi'an, Shaanxi 710072, China. E-mail: wangyiguang@nwpu.edu.cn*

The microstructural effects of SiC swelling, mechanisms of He diffusion and aggregation in C-rich SiC are studied using an in situ helium ion microscope. The additive carbon interface provides improved swelling resistance in SiC to ~270 nm, and defect formation is not observed until very high He implantation doses.

Continuous silicon carbide (SiC) fiber reinforced SiC matrix composites (SiC/SiC) are being considered as candidate structural materials for advanced fission reactors and future fusion reactors. Their primary advantages are their excellent mechanical properties and chemical stability at elevated temperatures, while maintaining low neutron activation and good radiation damage tolerance [1, 2]. With 14 MeV neutrons in a fusion reactor, SiC and other ceramic materials produce higher concentrations of transmutation gases (helium (He) and hydrogen (H)) than in ferritic steels and vanadium alloys [3, 4]. The reported He and H production rates in SiC in the first wall are approximately 130 and 40 atomic parts per million (appm), respectively, for a damage level of one displacement per atom (dpa) [3]. It is widely recognized that the limited solubility of He can enhance cavity formation in irradiated materials, degrade structural properties, and greatly affect the safety in power devices. However, a fundamental understanding of the physical process of He interacting in materials during irradiation is limited. The specific questions of interest include: What are the principal mechanisms to control the diffusion and aggregation of He? How are they influenced by the microstructure? How can the detrimental effects of He be diminished and handled via proper material design?

Over the last fifty years, a kind of in-situ facility has been investigated and developed to reveal the mechanisms and kinetics underlying damage production, accumulation and evolution, combined with a real-time transmission electron microscopy (TEM) observation with in situ ion irradiation [5]. Previous studies on He^+ irradiated SiC showed that He bubbles form above a specific temperature-dependent fluence and grow gradually as the implantation proceeds [6, 7]. Helium ion microscopes (HIM) are recently developed scanning ion microscopes based on a gas field ion source with high resolution (≤0.35 nm), which is close to the resolution in TEM. They also have low sample preparation requirements. Recent literature has given a detailed introduction to HIM [8]. In the present work, HIM was used as a powerful tool to bombard the sample surface by a focused He-ion beam of 30 keV while recording data in real-time. Extra phenol-formaldehyde (PF) resin was added to the SiC to imitate the common carbon (C)-rich surroundings in industrial SiC composites. SiC grain size and grain boundary effects were studied through a wide size range from tens of nanometers to several microns.

C-rich SiC with an atomic ratio of C/Si≈ 2.3 was prepared via solid-state sintering. Two *β*-SiC powders of 1 μm and 45~55 nm from Alfa Aesar were mixed with a mass ratio of 80:20. PF resin was used to homogeneously coat SiC powders using ethanol as a solvent. After low energy ball-milling at 80 revolutions per minute (rpm) for 70 h, the mixture powder was consolidated using a sing cycle with cold uniaxial pressing of 300 MPa and sintering at 1500 ^{o}C for 6 h in the argon atmosphere. The density of as-received sample was ~1.7 g/cm^3 by the Archimedes method. Fig. 1a shows two sharp peaks centered at 1357 and 1591 cm^{-1} using Raman spectroscopy, corresponding to the disorder induced D band and Raman-allowed G band in typical carbonaceous materials, respectively. By analyzing the I(D)/I(G) intensity ratio, the structure of pyrolytic carbon (PyC) from PF resin exhibits a similar disorder to nanocrystalline-graphite (NC-graphite) [9]. The surfaces of specimens were flatted and cleaned to ensure minimal contamination before being loaded into the main chamber of HIM.

The in-situ HIM (Orion Plus, Carl Zeiss SMT) was performed at room temperature (RT) in the Environmental Molecular Sciences Laboratory (EMSL) within the Pacific Northwest National Laboratory (PNNL). An acceleration voltage of 30 kV was used to irradiate the C-rich SiC specimens. Fig. 1b shows that the maximum irradiated depth of 30 keV He^+ was ~570 nm using the SRIM-2008 simulation with threshold displacement energies of 35 eV for Si and 20 eV for C atoms [10]. For a fluence of 1×10^{17} He/cm^2, the damage values are 0.457~1.248 dpa at 8-16 nm and 4.86 dpa at 288 nm of the damage peak. In-situ observation was achieved by using the internal patterning software to raster the focused He ion beam over an area of 1×1 or 2×2 μm^2 with an image size *P* of 1024×1120 pixels. A beam current about 20 pA was used and the dwell time per pixel *t* was selected as 10 μs or 20 μs to achieve the required fluence (ion/cm^2) based on its definition as the particle number *N* per area *A*:

$$\frac{dN}{dA}=\frac{\frac{I\times t}{ne}\times P}{A} \tag{1}$$

where *I* is the beam current, *n* is the charge number and *e* is the elementary charge of approximately 1.6×10^{-19} C. It suggests that appropriate dwell time and focused area are crucial to capture the slightest shift in surface morphology when other factors are constant.

SiC grains (see the convex regions) with sizes ranging from 35nm to 2μm were embedded in the PyC matrix by comparing the secondary electron (SE) and Rutherford backscattered ion (RBI) modes under HIM in Supplementary Fig. 1. Based on this, real-time observation of the SiC grain growth with different size at RT under in-situ 30 keV He^+ ion irradiation is shown in Fig. 2a to 2f. The focused area was 2×2 μm^2 and the dwell time was 10μs. A movie revealing the dynamic growth of SiC grains is shown in Supplemetary Video 1 to a total fluence of 5.605×10^{18} He^+/cm^2. Three SiC grains, A(>450 nm, in red contours), B(~270 nm, in blue contours) and C(~65 nm, in green contours) are selected as our subjects in this study. From

1.48×10^{17} to 2.22×10^{18} He^+/cm^2, the large grain A presents a typical swelling due to the fact that interstitial defects quickly move to the surface, while small grains B and C undergo no swelling or slowly shrinking under RT irradiation because the increasing proportion of grain boundary captures defects and re-emits them to annihilate with vacancies, showing an improved radiation resistance. F. Gao [11] and W. Jiang [12] have both found an "interface-driven-shrinking" in nanocrystalline SiC via theoretical and experimental approaches. However, in the previous study, the effects of structure and chemistry of the interface are overlooked. Moreover, there is a significant improvement in the critical size for interface-driven-shrinking by adding C into SiC, from 12 nm (simulated value [11]) or 3.8 nm (measured values [12]) to 270 nm.

To examine the growth rate in large SiC grains and the influence of diffusion and aggregation of He in more detail, we adjusted the dwell time to 20 μs and the focus area to $1\times1\mu m^2$. Fig. 3a-3h shows a series of in-situ HIM images containing two SiC microparticles and a C interface in between. The corresponding dynamic process at RT under 30 keV He^+ ion irradiation with a total fluence of 8.73×10^{18} He^+/cm^2 is given in Supplemetary Video 2. Grain growth occurs after necks are formed, thus the grain growth rate in SiC can be obtained from the measurement of the neck length (L) between the two SiC particles. The neck length (illustrated with the green dotted line) presents continuous growth in the first five frames of Video 2, from 0 to 1.13×10^{18} He^+/cm^2 (the neck will be out of the field of view from the sixth frame). And the corresponding swelling in SiC microparticles appears to be linear in Fig. 4a, with a growth rate of 11.37 %. At present, we cannot characterize the amorphous transformation using the in-situ HIM, but the above growth rate of SiC under He^+ ion irradiation is consistent with previous reports of 10.8 % in neutron-amorphized SiC under 343 K irradiation [13]. The implanted He tends to move to the sample surface for extremely low solubility in C-rich SiC, and a small cavity of ~6.5 nm first appears at the C interface at a fluence of 3.10×10^{18} He^{+}/ cm^2. As the irradiation proceeds, the small cavity becomes spherical in shape, such as defects A and B (circled in blue), and gradually grows to the maximum diameter as He gas releases from the cavity when it reaches saturation. The shrinkage leads to a sudden increase in the cavity mobility at the C interface. According to an earlier report [14], we attribute this type of defect, which moves freely on the surface of the C-rich SiC, to He interstitial bonds (He atoms on interstitial sites, type I) that diffuse quickly even below room temperature. The cavity size distribution was analyzed by Nano Measurer software. For type I cavity which gas-filled (a "bubble"), the maximum dimension was less than 40 nm (Fig.4b). Then He cavities move to the middle and coalesce into very large cavities (defects 1 and 2, circled in red) in the C interface with increasing radius from 18 to 80 nm at fluences from 6.47×10^{18} to 8.73×10^{18} He^{+}/cm^2. Since this type of defect is immobile and without a maximum dimension (type II), we believe that "bubble-to-void (cavities without gas)" transitions happen in the process. The subsequent implanted He interstitials are trapped by the voids to make the cavities even larger. According to the latest study by I.J. Beyerlein, et al.[15], this expansion-shrinkage in He cavities is a new morphological change when there exists grain boundaries or interfaces, and is driven by a competition between three kinds of pressures acting on the cavity. In the equilibrium condition, these pressures are:

$$P_{He} + P_V = P_c \qquad (2)$$

where P_{He} is the mechanical pressure of the trapped He gas, P_V is the osmotic pressure due to the flux of radiation-induced vacancies within the crystal to the cavity, and P_c is the capillary pressure arising from the surface energy of the cavity. P_{He} and P_V tend to expend the cavity while P_c tends to shrink it. Under RT irradiation, the flux of radiation-induced vacancies is very low because vacancies are practically immobile, which we hypothesize that P_v remains the same and could be ignored during the entire test. In the first stage, small cavities trap He gas to cause $P_{He}>P_c$, and expansion occurs. Carbon reconstructs with He ion beams due to the continuous loss of atoms[16], leading to an increase of surface energy. Thus, in the second stage, $P_{He}<P_c$, and shrinkage occurs. In the third stage, P_c stops increasing when C possesses the highest disorder since there is no more reconstruction. Meanwhile, the P_{He} in large cavities gradually increase as more and more He interstitials are trapped, $P_{He}>P_c$, and expansion occurs again. Fig. 4b shows the evolutions of defect diameters and defect number with fluences. The migration and coalescence processes, as well as the aforementioned expansion-shrinkage in He cavities, are illustrated in Fig. 5. The small cavity ~8 nm within SiC grain is first observed at a fluence of 7.88×10^{18} He^+/cm^2, which is much higher than that of the single crystal SiC (usually $\sim1\times10^{17}$ He^+/cm^2)[6, 17]. Combined with the aforementioned result in C interface (3.10×10^{18} He^+/cm^2), the threshold fluence for defect formation has greatly increased in C-rich SiC, which indicates that the radiation resistance can be improved by an additive C interface.

Conclusion

The in situ HIM observation of irradiation induced structural and defect evolutions in C-rich SiC has been performed for the first time. The high resolution of HIM offers the intriguing possibility to detect small cavities as small as 6.5 nm, and accurately measure the swelling rate in SiC grains. Grain boundaries are effective sinks for defects. The NC-graphite-like C interface in C-rich SiC effectively increases the swelling resistance in large SiC grains (<270nm). It also delays the emergence of He cavities and controls the number of cavities even at high He doses. Therefore, tailoring the interface with a C phase may offer a promising approach in SiC composite design for radiation resistance, and meet the demand for next-generation nuclear reactor applications.

Acknowledgements

W. Liu acknowledges support from the NPU's Exchange Funding.

Reference

1. P. Yvon and F. Carre, Structural materials challenges for advanced reactor systems, *J Nucl Mater*, 2009, **385**, 217-222.

2. S. J. Zinkle and J. T. Busby, Structural materials for fission & fusion energy *Mater Today*, 2009, **12**, 12-19.

3. L. L. Snead, R. H. Jones, A. Kohyama and P. Fenici, Status of silicon carbide composites for fusion, *J Nucl Mater*, 1996, **233**, 26-36.

4. T. Noda and M. Fujita, Effect of neutron spectra on the transmutation of first wall materials, *J Nucl Mater*, 1996, **233**, 1491-1495.

5. J. A. Hinks, A review of transmission electron microscopes with in situ ion irradiation, *Nucl Instrum Meth B*, 2009, **267**, 3652-3662.

6. K. Hojou, S. Furuno, K. N. Kushita, H. Otsu and K. Izui, In-situ observation of damage evolution in SiC crystals during He+ and H2+ dual-ion beam irradiation, *J Nucl Mater*, 1992, **191**, 583-587.

7. K. Hojou, S. Furuno, K. N. Kushita, H. Otsu, Y. Furuya and K. Izui, , In situ EELS and TEM observation of silicon carbide irradiated with helium ions at low temperature and successively annealed, *Nucl Instrum Meth B*, 1996, **116**, 382-388.

8. J. Notte, B. Ward, N. Economou, R. Hill, R. Percival, L. Farkas and S. McVey, An introduction to the helium ion microscope, *Aip Conf Proc*, 2007, **931**, 489-496.

9. A. C. Ferrari and J. Robertson, Raman spectroscopy of amorphous,

nanostructured, diamond–like carbon, and nanodiamond, *Philos T R Soc A,* 2004, **362**, 2477-2512.

10. J. F. Ziegler and J. P. Biersack, Stopping Power and Range of Ions in Matter, http://www.srim.org, 2008.
11. F. Gao, D. Chen, W. Y. Hu and W. J. Weber, Energy dissipation and defect generation in nanocrystalline silicon carbide, *Phys Rev B*, 2010, **81**, 184101-184108.
12. W. L. Jiang, L. Jiao and H. Y. Wang, Transition from Irradiation‐Induced Amorphization to Crystallization in Nanocrystalline Silicon Carbide, *J Am Ceram Soc*, 2011, **94**, 4127-4130.
13. L. L. Snead and S. J. Zinkle, Structural relaxation in amorphous silicon carbide, *Nucl Instrum Meth B*, 2002, **191**, 497-503.
14. H. Trinkaus and B. N. Singh, Helium accumulation in metals during irradiation–where do we stand?, *J Nucl Mater*, 2003, **323**, 229-242.
15. I. J. Beyerlein, A. Caro, M. J. Demkowicz, N. A. Mara, A. Misra and B. P. Uberuaga, Radiation damage tolerant nanomaterials, *Mater Today*, 2013, **16**, 443-449.
16. A. V. Krasheninnikov and F. Banhart, Engineering of nanostructured carbon materials with electron or ion beams, *Nat Mater*, 2007, **6**, 723-733.
17. S. J. Zinkle, Effect of H and He irradiation on cavity formation and blistering in ceramics, *Nucl Instrum Meth B*, 2012, **286**, 4-19.

Figures

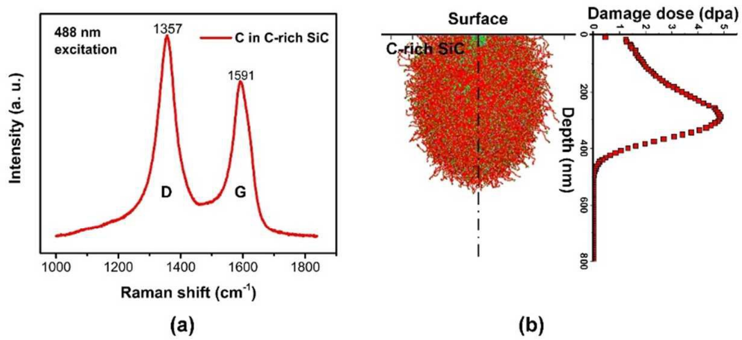

Fig. 1 (a) Raman spectrum of the prepared C-rich SiC using 100 mW, 488 nm excitation with a spot size of 1 μm, and (b) SRIM predicted collision(left) and damage profile(right) at XY longitudinal for the sample irradiated by 30 keV He^+ to a dose of 1×10^{17} /cm^2.

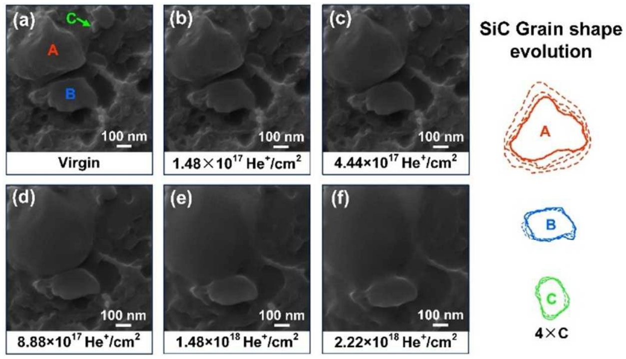

Fig. 2 Selected HIM images showing SiC grain shape evolutions to different doses: (a) 0, (b) 1.48×10^{17} He^{+}/cm^{2}, (c) 4.44×10^{17} He^{+}/cm^{2}, (d) 8.88×10^{17} He^{+}/cm^{2}, (e) 1.48×10^{18} He^{+}/cm^{2} and (f) 2.22×10^{18} He^{+}/cm^{2}. Three grains A (~450 nm), B (~270 nm) and C (~65 nm) use solid lines for original samples and dashed lines for irradiated samples.

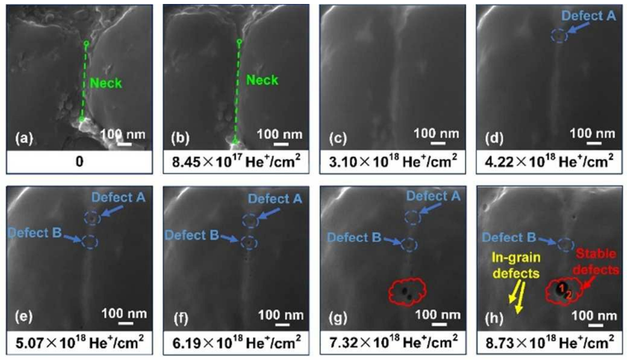

Fig. 3 He post-irradiation on Au-RT-irradiated sample in HIM focus on carbon interphase between two SiC micron-grains to different doses: (a) 0, (b) 8.45×10^{17} He^+/cm^2, (c) 3.10×10^{18} He^+/cm^2, (d) 4.22×10^{18} He^+/cm^2, (e) 5.07×10^{18} He^+/cm^2, (f) 6.19×10^{18} He^+/cm^2, (g) 7.32×10^{18} He^+/cm^2 and (h) 8.73×10^{18} He^+/cm^2.

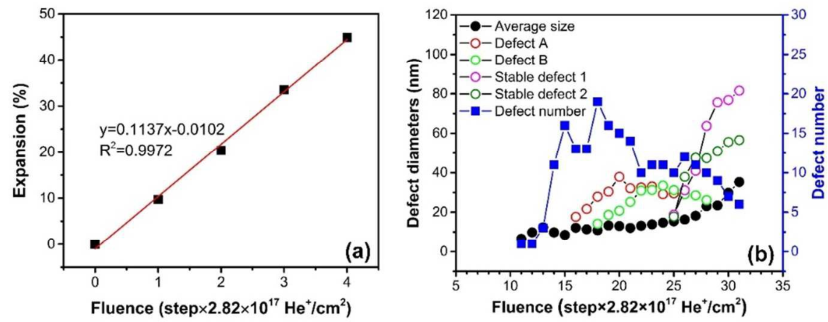

Fig. 4 (a) Expansion of micron-SiC under in-situ He irradiation, (b) Defect diameters and number with increasing fluence.

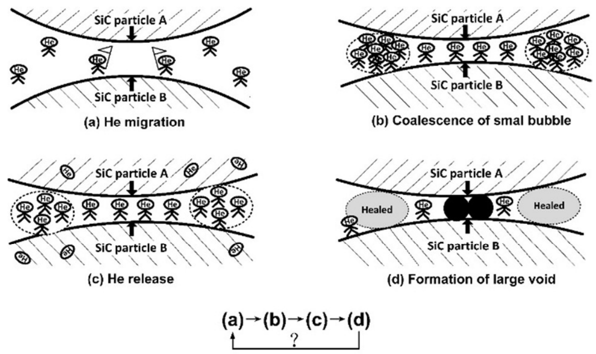

Fig. 5 Schematic illustrations of the helium cavities evolutions in C interface between two SiC grains under in-situ HIM.